Journal of Medicinal Chemistry

Article

pubs.acs.org/jmc

Discovery of GS-9669, a Thumb Site II Non-Nucleoside Inhibitor of NS5B for the Treatment of Genotype 1 Chronic Hepatitis C Infection

Scott E. Lazerwith,* Willard Lew, Jennifer Zhang, Philip Morganelli, Qi Liu, Eda Canales, Michael O. Clarke, Edward Doerffler, Daniel Byun, Michael Mertzman,† Hong Ye, Lee Chong, Lianhong Xu, Todd Appleby, Xiaowu Chen, Martijn Fenaux,‡ Ahmad Hashash,§ Stephanie A. Leavitt, Eric Mabery,∥ Mike Matles, Judy W. Mwangi, Yang Tian, Yu-Jen Lee, Jingyu Zhang, Christine Zhu, Bernard P. Murray, and William J. Watkins*

Gilead Sciences, Inc., 333 Lakeside Drive, Foster City, California 94404, United States

Supporting Information

ABSTRACT: Investigation of thiophene-2-carboxylic acid HCV NS5B site II inhibitors, guided by measurement of cell culture medium binding, revealed the structure−activity relationships for intrinsic cellular potency. The pharmacokinetic profile was enhanced through incorporation of heterocyclic ethers on the *N*-alkyl substituent. Hydroxyl groups were incorporated to modulate protein binding. Intrinsic potency was further improved through enantiospecific introduction of an olefin in the *N*-acyl motif, resulting in the discovery of the phase 2 clinical candidate GS-9669. The unexpected activity of this compound against the clinically relevant NS5B M423T mutant, relative to the wild type, was shown to arise from both the *N*-alkyl substituent and the *N*-acyl group.

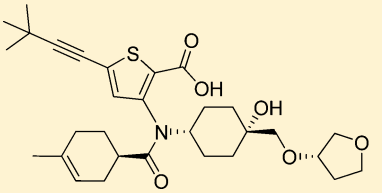

53 (GS-9669)

INTRODUCTION

In recent years, as clinical data from numerous new small-molecule hepatitis C virus (HCV) inhibitors with different modes of action have been reported, it has become increasingly clear that interferon-based treatment regimens will soon be supplanted by all-oral combinations of direct-acting antiviral agents.[1,2] In this context, regimens that deliver the maximum benefit to patients in terms of efficacy and brevity of treatment duration will be those that consist of multiple agents targeting different inhibitory mechanisms with complementary resistance profiles. An ideal combination would include drugs with once daily dosing schedules that could be coformulated into a single tablet regimen.[3]

One of the most well-studied targets for the inhibition of HCV replication by small molecules is the viral polymerase NS5B.[4] Inhibitors fall into two broad categories: nucleos(t)ide analogues that become incorporated into the nascent RNA chain and result in defective elongation, and non-nucleoside inhibitors whose activity results from binding at diverse allosteric sites, four of which have been shown to be exploitable for clinical efficacy. Among these is thumb site II, located ∼30 Å from the active site. Screening hits from various HCV discovery programs[5−10] are now known to act by binding at this site, and their optimization[11−18] has resulted in the identification of several clinical candidates, three of which (covering disparate chemotypes) are illustrated in Figure 1. The medicinal chemistry optimization programs leading to HCV-371 (**1**)[5] and filibuvir (**2**)[16] have been published, but the structure of lomibuvir (**3**) was revealed only upon recent assignment of a nonproprietary name.[19] All of these inhibitors retain useful levels of activity only in genotype (GT) 1 HCV, although a recent publication has reported compounds with $EC_{50} \leq 80$ nM against GTs 2−6.[20] Characteristic of antiviral agents with this mechanism of action is the emergence of NS5B M423T as a resistant mutant, both clinically and in in vitro studies.[4]

The attractiveness of NS5B thumb site II inhibitors for use in combination regimens was increased by early reports of clinical results with **2**, which demonstrated a 2.3 $\log_{10}$ reduction in HCV RNA in plasma when dosed as monotherapy at 700 mg twice daily for 8 days in GT 1 infected patients,[21] and by **3** (then referred to as VCH-222), which achieved a 3.7 $\log_{10}$ reduction in plasma viral RNA after 3 days of treatment at 750 mg twice daily.[22]

As part of a broad HCV discovery effort, we initiated a program to discover a new NS5B thumb site II inhibitor for use in future single-tablet regimens. Such an agent would be more potent than previous examples (to minimize dose), would exhibit improved pharmacokinetics (to enable once-daily dosing), and would have physicochemical properties compatible with convenient coformulation with other agents. In view of the clinical potency of **3** and the relatively small molecular size of the class, we chose to explore the thiophene-2-carboxylic acids for optimization.

Special Issue: HCV Therapies

Received: September 13, 2013

dx.doi.org/10.1021/jm401420j | *J. Med. Chem.* XXXX, XXX, XXX−XXX

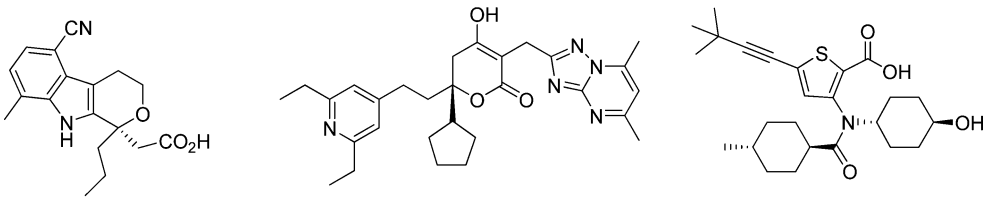

1 (HCV-371) **2** (Filibuvir) **3** (Lomibuvir)

Figure 1. Structures of selected clinical candidates.

Scheme 1. Generalized Synthetic Route[a]

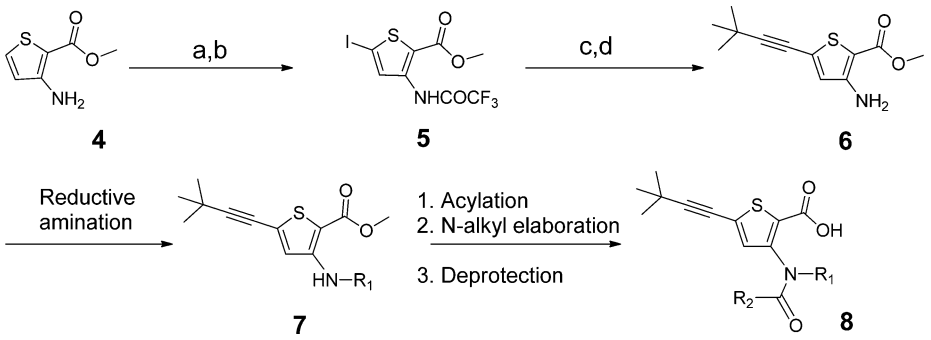

[a]Reagents and conditions: (a) trifluoroacetic anhydride; (b) LDA, then I_2; (c) *t*-Bu acetylene, $Pd(Ph)_2Cl_2$, CuI; (d) K_2CO_3.

METHODS AND RESULTS

Potency was determined using subgenomic GT 1a and 1b replicon assays[23−25] in a medium containing 10% fetal bovine serum. To establish that the observed replicon inhibition was specific, cytotoxicity was determined in the replicon cell line in parallel with potency, and all the compounds in this article exhibited $CC_{50} > 20\ \mu M$. Cytotoxicity in the MT4 cell line was measured as previously described.[25] In order to better interpret structure−activity relationships, the unbound fraction in both cell culture medium (CCM) and human plasma was measured by dialysis for many compounds. Intrinsic potency was defined as [replicon EC_{50} × free fraction in CCM]. Plasma-adjusted potency was defined as [replicon EC_{50} × (plasma/CCM free fraction ratio)] and was used to estimate the potency expected in a clinical setting.

Most of the new analogues were synthesized using the general synthetic route shown in Scheme 1, which begins with the amino protection and selective iodination of commercially available methyl 3-aminothiophene-2-carboxylate (**4**) to afford the 5-iodothiophene **5**. Sonagashira coupling with *tert*-butylacetylene and deprotection give the versatile 3-aminothiophene **6**. This intermediate is then monoalkylated via reductive amination, forming **7**, and acylated with an acid chloride. The resulting hindered amide may then be subject to further elaboration of the *N*-alkyl substituent and is finally hydrolyzed to the desired carboxylic acid **8**.

The observed and intrinsic potencies of a concise set of initial analogues exploring the impact of key substituents upon activity are reported in Table 1.

In general for compounds in this series, activity against the GT 1a replicon was weaker than for GT 1b, and in order to maximize activity in all GT 1 patients, further optimization was therefore directed toward GT 1a. Comparison of **9**[14] and **10**[26] illustrates the benefit of replacement of the 5-phenyl substituent with the more recently discovered *tert*-butylacetylene moiety, resulting in a 30-fold improvement in intrinsic potency. The intrinsic potencies of **3**, **11**, and **12** are broadly similar to **10**, with the differences in observed activity largely attributable to changes in CCM binding, as might be expected by inspection of the cocrystal structure of **10** bound in thumb site II (Figure 2) in which it is evident that the *N*-alkyl substituent is directed away from the protein. The requirement for branching of the *N*-alkyl substituent in order to confer high levels of potency[14] was

Table 1. CCM Binding and HCV Replicon Activity of Initial Analogues

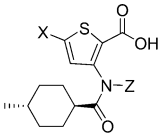

Cmpd	X	Z	CCM f_u[a]	GT 1b EC_{50}[b] (nM)	GT 1a EC_{50} (nM)	
					Observed	Intrinsic
9	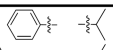		0.08	593	2,100	170
10	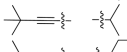		0.06	26	90	5.5
3	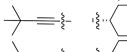		0.19	6	13	2.8
11	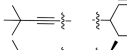		0.71	2	15	11
12	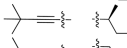		0.22	7	15	3.3
13	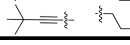		ND[c]	78	304	ND

[a]f_u: fraction unbound. [b]Huh7 CC_{50} for all the analogues reported herein was ≥20 μM. [c]ND: not determined.

corroborated in the hydroxyl-containing analogues **12** and **13**. Neither of the methyl groups in the *N*-alkyl substituent of **10** are in van der Waals contact with the protein; we infer that the increased conformational rigidity around the amide plays a significant role in the potency increase. Consistent with this, atropisomers were observable in the proton NMR spectra for analogues bearing chiral N-substituents (such as **12**).[27] A similar phenomenon has recently been reported in a closely related series of anthranilates.[28] The importance of the amide as a polar and atom-efficient scaffolding element for positioning of the acyl moiety relative to the thiophene core has previously been emphasized.[29,30]

Noting the similar intrinsic potency of compounds (**3** and **10**−**12**), which vary only in the apparently solvent exposed *N*-alkyl substituent, we anticipated that a broader investigation in this region of the structure might enable modulation of other properties. Examples of further variations at this position are listed in Table 2.

The results for compounds **14**−**17** demonstrate that despite the apparent lack of direct contact with Δ21 NS5B protein (Figure 2), not

dx.doi.org/10.1021/jm401420j | J. Med. Chem. XXXX, XXX, XXX−XXX

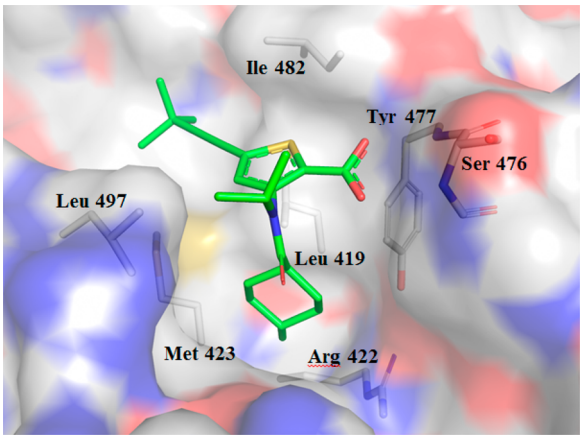

Figure 2. Cocrystal structure of **10** bound to GT 1b NS5B Δ21.

Table 2. CCM Binding and HCV Replicon Activity of Further *N*-Alkyl Substituents

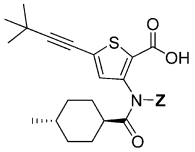

Cmpd	Z	CCM f_u	GT 1a EC_{50} (nM)	
			Observed	Intrinsic
14	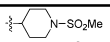	0.17	51	8.7
15	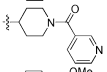	0.23	183	43
16	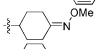	0.07	88	6.1
17	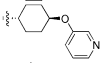	0.03	128	3.6
18	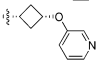	0.04	156	6.4
19	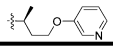	0.02	102	2.4

all branched *N*-alkyl substituents confer the same level of intrinsic potency in the cellular replicon assay (where NS5B forms part of a multimeric protein assembly known as the replicase complex).[31] The pyridyl ether **17**, however, displayed intrinsic potency similar to the best analogues in Table 1, and analogues **18** and **19** illustrate the structure−activity relationships (SAR) of linking units of this motif with the rest of the molecule. Intrinsic potency was slightly diminished in the case of the cyclobutane linker but could be maintained through use of a branched, linear chain.

Compound **17** was profiled in drug metabolism and pharmacokinetic studies, and on the basis of the promising stability in microsomal assays[25] and long mean residence time in rat, a variety of related ethers was explored, as summarized in Table 3.

Both trans- and cis-4-substituted cyclohexyl ethers (and thioethers, data not shown) provided analogues retaining intrinsic potency across a range of heterocycles. Curiously, the mean residence times of the cis analogues in rat were short and inconsistent with predictions from in vitro metabolism assays (**20**, **25**). By contrast, the trans analogues were well-behaved in vivo, resulting in long mean residence times. The predicted human hepatic extraction ratios of several of these analogues, including the saturated heterocyclic ether **27**, were lower than could be readily measured in in vitro assays.

In order to explore the potential of the *tert*-butyl motif for further optimization, variants at this position in the context of the pyridazonyl ether **24** were briefly explored (vide infra, Table 4). These analogues were prepared as shown in Scheme 2. The advanced 5-iodothiophene intermediate **28** was treated with isopropylmagnesium bromide

Table 3. Intrinsic Potency, in Vitro Metabolism, and Rat Pharmacokinetics of 17 and 20−27

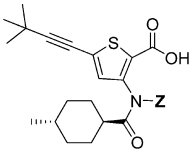

Cmpd	Z	GT 1a EC_{50} (nM)		Predicted hepatic extraction ratio (%)[a]		Rat mean residence time (h)
		Observed	Intrinsic	Human	Rat	
17	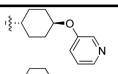	128	3.6	13	11	3.4
20	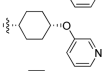	45	1.2	28	49	0.2
21	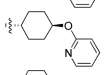	297	2.5	<7	<5	5.0
22	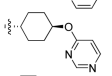	75	2.8	<7	<5	7.1
23	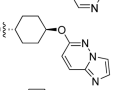	192	1.3	<7	11	6.2
24	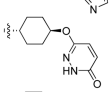	39	3.5	11	6	1.6
25	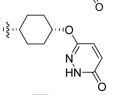	24	2.6	<7	<5	0.5
26	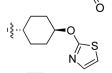	84	1.5	14	<5	2.8
27	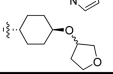	55	8.1	<7	<5	3.5

[a]From liver microsomal stability assays with cofactors for glucuronidation added.

Table 4. Survey of *tert*-Butyl Variants

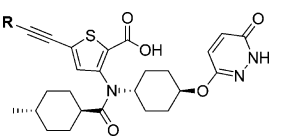

Cmpd	R	GT 1a EC_{50} (nM)			Predicted human hepatic extraction ratio (%)
		Observed	Intrinsic	Plasma-adjusted	
24		39	3.5	285	11
33		51	4.9	516	<7
34		61	6.9	751	<7
35		120	2.7	607	14

followed by an appropriate Weinreb amide, giving ketone **29**. After hydroxyl deprotection, Seyferth−Gilbert homologation[32] using Bestmann's reagent[33] generated the alkyne **31**. Generation of the pyridazonyl ether **32** was accomplished by S_NAr reaction of the alkoxide of **31** with 3,6-dichloropyridazine and subsequent hydrolysis.

The utility of the trifluoromethylcyclopropyl group as a metabolically stable *tert*-butyl replacement has recently been highlighted.[34] While both **33** and **34** did indeed exhibit improved stability, plasma-adjusted potency was compromised, and the cyclobutyl analogue **35** was worse in both respects.

dx.doi.org/10.1021/jm401420j | J. Med. Chem. XXXX, XXX, XXX−XXX

Scheme 2. General Synthetic Route to Alkyne Analogues[a]

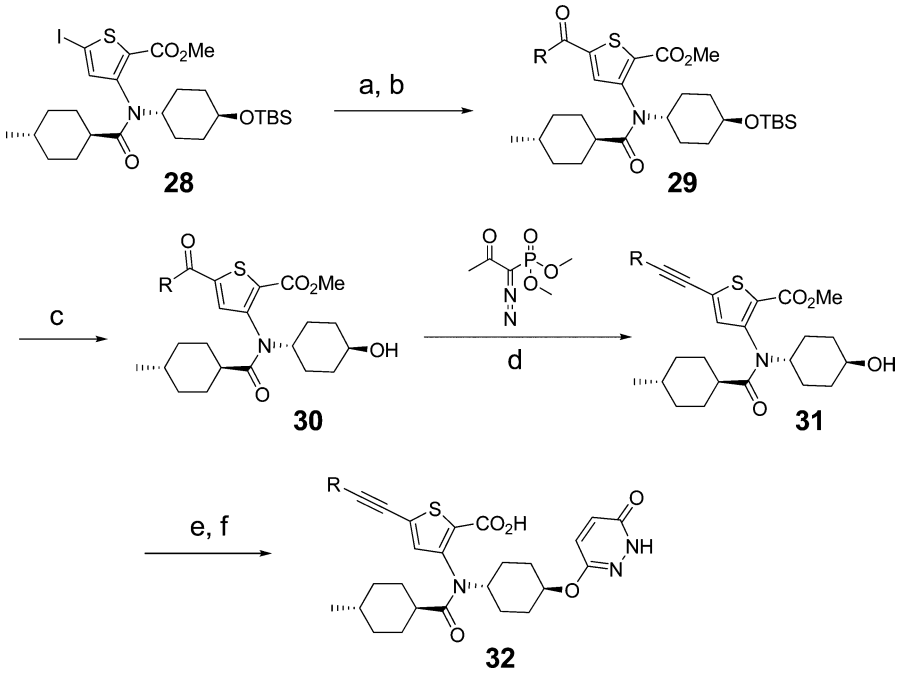

[a]Reagents and conditions: (a) *i*-PrMgBr; (b) RCON(Me)OMe; (c) TFA; (d) K_2CO_3, MeOH; (e) NaH, then 3,6-dichloropyridazine; (f) NaOAc, AcOH.

It is evident from a comparison of the observed and intrinsic potencies in Table 3 that the degree of CCM binding varied considerably across these analogues, and an assessment of the impact of human plasma binding and its association with log *D* was informative. As a preliminary safety screen, we also assessed the cytotoxicity of the analogues in the rapidly dividing lymphoid MT4 cell line, as summarized in Table 5.

Table 5. log *D*, Plasma-Adjusted Potency, and Intrinsic Cytotoxicity for Selected Analogues

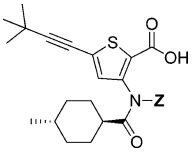

Cmpd	Z	LogD	Plasma-adjusted GT 1a EC_{50} (nM)	Intrinsic MT4 CC_{50} (nM)
21	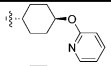	3.0	1,053	100
22	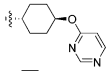	2.3	1,391	599
23	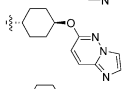	2.4	1,130	133
24	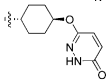	2.0	285	1,481
25	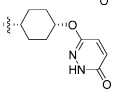	1.8	277	2,167
27	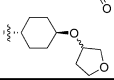	2.3	749	3,072

A trend was noted in which the more lipophilic heteroaromatic ethers tended to exhibit greater intrinsic cytotoxicity and less favorable plasma-adjusted potency. Over 140 *N*-alkyl substituents of this type were examined in a search to combine potency, low cytoxicity, metabolic stability, and an in vivo pharmacokinetic profile into a single compound. Ultimately, the results with the saturated heterocyclic analogue **27** led to further exploration of this subset of ether-linked compounds, with an emphasis on reduction in log *D* to further optimize plasma-adjusted potency (Table 6).

Variation of the heterocycle ring size gave analogues with similar intrinsic potency, but the microsomal stability of **36** was reduced (predicted human hepatic extraction 16%) and the plasma-adjusted potency of **37** was compromised. The addition of hydroxyl groups produced diverse outcomes: on an extended alkynyl motif (**38**) intrinsic potency was reduced and the mean residence time in rat was very short (despite predicted rat hepatic extraction of only 8%); adjacent to the amide carbonyl group (**39**)[11] no significant impact on log *D* resulted and the in vivo profile was compromised; and when incorporated on the amide *N*-alkyl substituent (**40**) resulted in an analogue that exhibited a rat mean residence time similar to that of **27** but with improved plasma-adjusted potency. As in earlier cases, the rat mean residence time was exquisitely sensitive to the stereochemistry of the *N*-alkyl substituent (**41** vs **40**).

The stringent SAR of the amide acyl group, which binds in the lipophilic pocket lined by L419, R422, M423, and W528,[35] was illustrated in earlier work[14] where it was reported that a 4-methyl substituent was required to be present and equatorial on the cyclohexyl ring in order to achieve submicromolar levels of activity in the replicon. We next elected to explore this motif further in an effort to improve intrinsic potency (Table 7).

Correction for CCM binding reveals that the magnitude of the increase upon incorporation of the equatorial 4-methyl substituent (**10** vs **42**) is ~100-fold, typical of the maximum observed in a survey of all methyl group effects and consistent with its placement deep in the hydrophobic pocket.[36] The sensitivity of the SAR for the 4-substituent of the cyclohexyl motif was further confirmed by the weaker activity of **43** and **44**. The dramatic loss in activity in **45** likely reflects the known intolerance for any axial 4-substituent. The intrinsic potency of the unsubstituted cycloheptyl variant **46** was similar to that of the

dx.doi.org/10.1021/jm401420j | J. Med. Chem. XXXX, XXX, XXX–XXX

Table 6. Profiles of Saturated Heterocyclic Ethers

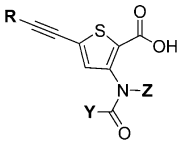

Cmpd	R	Y	Z	LogD	GT 1a EC_{50} (nM) Intrinsic	GT 1a EC_{50} (nM) Plasma-adjusted	Intrinsic MT4 CC_{50} (nM)	Rat mean residence time (h)
27				2.3	4.3	749	3,072	3.5
36				2.6	4.3	102	8,347	ND
37				2.4	2.4	1,833	1,988	ND
38	HO			1.6	6.1	167	31,251	0.4
39		OH		2.2	2.0	138	11,611	1.9
40			OH	2.4	2.2	208	8,982	3.8
41			OH	ND[a]	4.3	191	18,072	0.2

[a]ND: not determined.

Table 7. CCM Binding and HCV Replicon Activity of Acyl Variants

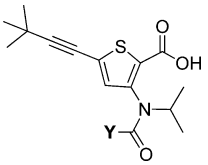

Cmpd	Y	CCM f_u	GT 1a EC_{50} (nM) Observed	GT 1a EC_{50} (nM) Intrinsic
10		0.06	90	5.5
42		0.18	2,800	500
43	Cl	0.14	315	44
44	F	0.18	169	31
45	F, F	0.40	32,120	12,820
46		0.11	2,020	225
47	H, H	0.04	4,680	206
48		0.08	6,190	483
49		0.05	1,620	88
50		0.08	773	65
51		0.08	45	3.7
52		0.07	31	2.2

cyclohexane **42**, but attempts to increase potency through modulation of conformation or the addition of an extra carbon at the distal end of the ring (**47**–**49**) were unsuccessful. The introduction of unsaturation into the six-membered ring resulted in remarkably dissimilar outcomes: although the conjugated cyclohexene **50** was much less active than **10**, the unsaturated isomers **51** and **52** demonstrated a small but reproducible improvement in both the observed and intrinsic potency, with the *R* enantiomer the more active of the two.

Finally, when the preferred unsaturated acyl motif ((*R*)-methyl-cyclohexenyl from compound **52**) was combined with the previously optimized *N*-alkyl substituent (from compound **40**), the resulting compound (**53**) was shown to have a favorable profile including high potency, high metabolic stability in vitro, and an encouraging mean residence time in rat (Table 8). A broader summary of its preclinical

Table 8. Profile of 53

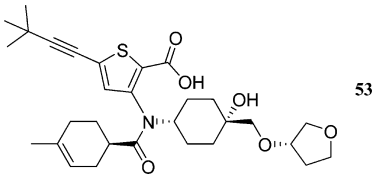

GT 1a EC_{50} (nM) observed	GT 1a EC_{50} (nM) intrinsic	GT 1a EC_{50} (nM) plasma-adjusted	intrinsic MT4 CC_{50} (nM)	predicted hepatic extraction ratio (%) human	predicted hepatic extraction ratio (%) rat	rat mean residence time (h)
11	2.9	128	12138	<7	<5	2.7

characteristics has been previously described.[25] **53** (GS-9669) is currently being evaluated in phase 2 clinical combination studies for chronic HCV.

Compound **53** retains a high level of activity against the NS5B M423T mutation.[25] In order to explore the contribution of the different substituents to this phenomenon, side-by-side transient transfection GT 1b assays[24] with wild type (WT) and M423T NS5B replicons were performed on a concise set of analogues, with the results shown in Table 9.

dx.doi.org/10.1021/jm401420j | J. Med. Chem. XXXX, XXX, XXX–XXX

Table 9. Transient Transfection Results with WT and M423T NS5B Replicons

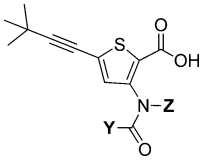

Cmpd	Y	Z	GT 1b EC_{50} (nM)		M423T / WT fold shift
			WT	M423T	
10			26	293	11
40		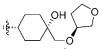	12	47	4
52			8	40	5
53		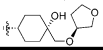	6	14	2

Both the *N*-alkyl substituent and the acyl motif that are incorporated in **53** confer greater activity against the mutant than would be anticipated based on the profile of **10**, as demonstrated by the reduction in fold shift for **40** and **52**, respectively. The unexpected contribution of the *N*-alkyl substituent further highlights the unknown aspects of this region of the structure in the context of the replicase complex in cells. The combination of the two motifs in **53** provides an additive effect, resulting in a minimal reduction in activity against this clinically relevant mutation.

The synthetic route to **53** (Scheme 3) utilized intermediate **6** (Scheme 1), which was subjected to a reductive amination with the monoketal of 1,4-cyclohexanedione. Secondary amine **54** was then acylated under mild buffered conditions with the acid chloride of (*R*)-4-methylcyclohex-3-enecarboxylic acid[37] resulting in the fully substituted amide **55**. Ketal deprotection followed by Corey–Chaykovsky epoxidation gave epoxide **56** stereoselectively. Finally, ester saponification and epoxide opening with (*S*)-tetrahydrofuran-3-ol afforded the desired compound.

CONCLUSION

Investigation of thiophene 2-carboxylic acid HCV NS5B site II inhibitors, guided by measurement of CCM binding, revealed the SAR for intrinsic cellular potency. The pharmacokinetic profile was enhanced through incorporation of heterocyclic ethers on the *N*-alkyl substituent. Hydroxyl groups were added to modulate lipophilicity, thereby reducing protein binding. Intrinsic potency was further improved through enantiospecific introduction of an olefin in the acyl motif, resulting in the discovery of **53** (GS-9669). The surprising activity of this compound against M423T was shown to arise from both the *N*-alkyl substituent and the acyl group. In phase 1 clinical studies, compound **53** exhibited a median half-life of 6–7 h in chronic HCV patients and produced a 3.6 $\log_{10}$ reduction in plasma viral RNA after 3 days of treatment at 500 mg once daily.[38] This compound is currently being evaluated in phase 2 clinical studies in combination with other direct acting anti-HCV agents.

EXPERIMENTAL SECTION

All commercial reagents were used as provided. Flash chromatography was performed using ISCO Combiflash Companion purification system with RediSep R_f prepacked silica gel cartridges supplied by Teledyne Isco. ^{1}H NMR spectra were recorded on a Varian Inova 300 MHz, a Varina Mercury Plus 400 MHz, or a Bruker Advance 400 MHz spectrometer. Proton chemical shifts are reported in ppm from an internal standard or residual solvent. Purity of tested compounds was assessed to be at least 95% by HPLC analysis unless indicated otherwise. A Gemini C18 110 Å column (50 mm × 4.6 mm, 5 μm particle size) was used with gradient elution of acetonitrile in water, with detection at 254 nm wavelength. For all samples 0.1% TFA was added to both eluents. Mass spectrometry was performed on a Finnigan LCQ Advantage MAX mass spectrometer with a Thermo LCQ Advantage HPLC. The samples were run on a Phenomenex Gemini, C_{18} column using reverse phase chromatography and acetonitrile/water containing 0.1% acetic acid as eluent.

5-(3,3-Dimethylbut-1-ynyl)-3-((*R*)-*N*-((1*R*,4*S*)-4-hydroxy-4-(((*S*)-tetrahydrofuran-3-yloxy)methyl)cyclohexyl)-4-methylcyclohex-3-enecarboxamido)thiophene-2-carboxylic Acid (53). *Scheme 1, Steps a and b.* Trifluoroacetic anhydride (18 mL, 27.3 g, 130 mmol) was added dropwise to a solution of methyl 3-aminothiophene-2-carboxylate (20 g, 127 mmol) in ethyl ether (140 mL), stirring at −5 to −10 °C over 1 h. The resulting suspension was slowly warmed to room temperature with vigorous stirring overnight. The mixture was washed successively with 1 N aqueous HCl (60 mL), water (50 mL), and brine (50 mL) and dried over anhydrous Na_2SO_4.

Scheme 3. Synthesis of GS-9669[a]

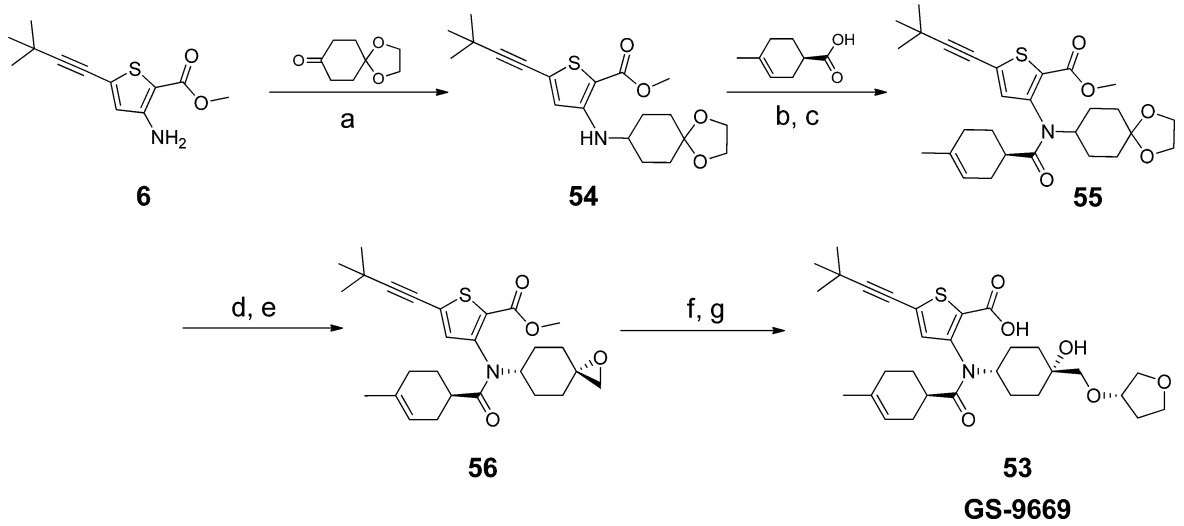

[a]Reagents and conditions: (a) Bu_2SnCl_2, $PhSiH_3$; (b) oxalyl chloride; (c) K_3PO_4; (d) HCl; (e) $Me_3SO^+I^-$, NaH; (f) LiOH; (g) (*S*)-tetrahydrofuran-3-ol, KO*t*-Bu.

dx.doi.org/10.1021/jm401420j | J. Med. Chem. XXXX, XXX, XXX–XXX

Concentration in vacuo and trituration with diethyl ether gave a white solid which was used without purification (32 g, 99% yield). ^{1}H NMR (400 MHz, DMSO-d_6): δ 11.2 (s, 1H), 8.02 (d, J = 5.6 Hz, 1H), 7.71 (d, J = 5.2 Hz, 1H), 3.85 (s, 3H).

n-BuLi (2.5 M in hexane, 123 mL, 308 mmol) was added dropwise over 30 min to a solution of diisopropylethylamine (47 mL, 355 mmol) in anhydrous THF (300 mL) at −78 °C under argon. The mixture was stirred for 30 min at −78 °C. To this freshly prepared LDA solution, methyl 3-(2,2,2-trifluoroacetamido)thiophene-2-carboxylate from the previous step (23.6 g, 93 mmol) was added dropwise as a solution in THF (110 mL) over 40 min. The resulting mixture was stirred at −78 °C for 1 h, and then a solution of I_2 (35.5 g, 140 mmol) in THF (110 mL) was added over 1 h. The reaction mixture was continually stirred for another 1 h at −78 °C, quenched with saturated aqueous NH_4Cl (500 mL), and extracted with EtOAc (800 mL). The organic layer was separated and washed with 15% aqueous $Na_2S_2O_3$ (2 × 500 mL), 10% citric acid (500 mL), brine (500 mL), and dried over anhydrous $MgSO_4$. Concentration in vacuo and purification by silica gel flash column (EtOAc/hexanes) gave methyl 5-iodo-3-(2,2,2-trifluoroacetamido)thiophene-2-carboxylate (**5**) as a gray solid (23.2 g, 70% yield). ^{1}H NMR (400 MHz, $CDCl_3$): δ 11.2 (s, 1H), 8.01 (s, 1H), 3.84 (s, 3H).

Scheme 1, Steps c and d. A 500 mL three-neck flask equipped with a thermometer and a stirrer was charged with **5** (23.2 g, 61 mmol), CuI (2.33 g, 12.2 mmol), *tert*-butylacetylene (10.0 g, 122 mmol), $Pd(PPh_3)_2Cl_2$ (4.29 g, 6.1 mmol), DMF (300 mL), and Et_3N (4.3 g). The mixture was stirred at 80 °C under nitrogen for 1.5 h, cooled to room temperature, diluted with EtOAc (1 L), and filtered to remove solids. The filtrate was washed with water (500 mL), brine (500 mL) and dried over anhydrous Na_2SO_4. Concentration in vacuo and purification by flash chromatography (EtOAc/hexanes) gave methyl 5-(3,3-dimethylbut-1-ynyl)-3-(2,2,2-trifluoroacetamido)thiophene-2-carboxylate as a pale yellow solid (12.3 g, 60% yield). ^{1}H NMR (400 MHz, $CDCl_3$): δ 11.1 (s, 1H), 8.00 (s, 1H), 3.92 (s, 3H), 1.32 (s, 9H). MS (ESI^-) m/z: 332 $[M - 1]^-$.

A mixture of methyl 5-(3,3-dimethylbut-1-ynyl)-3-(2,2,2-trifluoroacetamido)thiophene-2-carboxylate (12.3 g, 36.8 mmol) and K_2CO_3 (10.2 g, 73.6 mmol) in methanol (70 mL), THF (70 mL), and H_2O (70 mL) was stirred at room temperature for 2.5 h and neutralized with 1 N HCl to pH 8. The mixture was concentrated to remove the volatile solvents, and the aqueous solution was extracted with EtOAc (500 mL). The organic layer was dried over anhydrous Na_2SO_4 and concentrated to dryness. The residue obtained was triturated with petroleum ether and dried in a vacuum oven to give methyl 3-amino-5-(3,3-dimethylbut-1-ynyl)thiophene-2-carboxylate (**6**) as a white solid (7.9 g, 91% yield). ^{1}H NMR (400 MHz, DMSO-d_6): δ 6.62 (s, 1H), 6.54 (s, broad, 2H), 3.70 (s, 3H), 1.27 (s, 9H). MS (ESI^+) m/z: 238 $[M + 1]^+$.

Scheme 3, Step a. Dibutyltin dichloride (3.03 g, 0.1 mmol) was added to compound **6** (23.7g, 100 mmol) and 1,4-dioxa-spiro[4.5]-decan-8-one (18.7g, 120 mmol) in THF (20 mL) and DMF (10 mL). After 5 min, phenylsilane (13.6 mL, 111 mmol) was added and the resulting mixture was stirred overnight. Ethyl acetate was added, and the reaction mixture was washed with 5% LiCl solution and brine. The organic phase was separated and dried over anhydrous Na_2SO_4. After concentration, the crude material was purified by flash chromatography, eluting with ethyl acetate, to give methyl 3-(1,4-dioxaspiro[4.5]-decan-8-ylamino)-5-(3,3-dimethylbut-1-ynyl)thiophene-2-carboxylate (**54**) as a light yellow solid (32.1 g, 89% yield). ^{1}H NMR (400 MHz, DMSO-d_6): δ 7.036 (s, 1H), 6.671 (d, J = 8.4 Hz, 1H), 3.86 (m, 4H), 3.71 (s, 1H), 3.58 (m, 1H), 1.85 (m, 2H), 1.62 (m, 4H), 1.47 (m, 2H), 1.28 (s, 9H). MS (ESI^+) m/z: 378 $[M + 1]^+$.

Scheme 3, Steps b and c. (1*R*)-4-Methylcyclohex-3-enecarboxylic acid[36] (4.00 g, 28.5 mmol, azeotropically dried by evaporation of a toluene solution) and freshly ground potassium phosphate tribasic (7.55 g, 35.6 mmol) were suspended in dichloromethane (81 mL), treated with DMF (0.120 mL), and placed in a 0 °C bath. After 5 min, the mixture was treated portionwise over 15 min with oxalyl chloride (8.10 mL, 85.5 mmol). After the mixture was stirred for 1 h, the heterogeneous mixture was quickly filtered through a small pad of Celite, rinsed with dichloromethane, and concentrated to give (1*R*)-4-methylcyclohex-3-enecarboxylic acid chloride (4.28 g, 95% yield), which was used immediately in the next step.

(1*R*)-4-Methylcyclohex-3-enecarboxylic acid chloride (4.28 g, 27.0 mmol), **54** (3.40 g, 9.0 mmol), and potassium phosphate tribasic (5.73 g, 27.0 mmol) were suspended in dichloroethane (22.5 mL), placed in an oil bath at 80 °C, and stirred under nitrogen. After 6 h, an additional 5 mL of dichloroethane was added. After 16 h, the mixture was cooled and partitioned between ethyl acetate and water. The organic layer was separated and washed with water and brine and dried over anhydrous Na_2SO_4, filtered, and concentrated. Flash chromatography (EtOAc/hexanes) afforded the desired methyl 5-(3,3-dimethylbut-1-ynyl)-3-((1*R*)-4-methyl-*N*-(1,4-dioxaspiro[4.5]decan-8-yl)cyclohex-3-enecarboxamido)thiophene-2-carboxylate (**55**) as a white foam (3.31 g, 74% yield). ^{1}H NMR (400 MHz, DMSO-d_6): δ 7.29 (d, J = 18.9 Hz, 1H), 5.25 (br d, J = 14.1 Hz, 1H), 4.42 (br t, J = 12.2 Hz, 1H), 3.87−3.65 (m, 7H), 2.30−1.53 (m, 10H), 1.51 (s, 3H), 1.44−1.32 (m, 1H), 1.30 (d, J = 2.7 Hz, 9H), 1.06−0.89 (m, 1H).

Scheme 3, Steps d and e. **55** (3.31 g, 6.63 mmol) was dissolved in THF (53 mL), and 4 M HCl (26.5 mL) was added. The reaction mixture was heated to 45 °C and stirred for 2 h. Ethyl acetate was added, and the organic layer was separated. The aqueous was extracted again with ethyl acetate, and the combined organics were washed with saturated aqueous sodium bicarbonate, water, and brine. The organic layer was dried over anhydrous Na_2SO_4, filtered, and concentrated to afford 5-(3,3-dimethylbut-1-ynyl)-3-[(1*R*)-4-methylcyclohex-3-enecarbonyl)-(4-oxocyclohexyl)amino]thiophene-2-carboxylic acid methyl ester as a white foam (3.03 g, 100% yield).

A solution of trimethylsulfoxonium chloride (1.07 g, 8.31 mmol) in DMSO (24 mL) was treated with sodium hydride (0.293 g, 60% oil dispersion, 7.32 mmol) portionwise over 10 min and stirred at ambient temperature for 20 min. 5-(3,3-Dimethylbut-1-ynyl)-3-[(1*R*)-4-methylcyclohex-3-enecarbonyl)-(4-oxocyclohexyl)amino]thiophene-2-carboxylic acid methyl ester (3.03 g, 6.65 mmol) in THF (24 mL) was added dropwise over 5 min, and the reaction mixture was stirred for 45 min. The orange solution was acidified to pH 3 with 5% citric acid and partitioned between water and ethyl acetate. The organic layer was separated, and the aqueous layer was extracted again with ethyl acetate. The combined organic extracts were washed with 5% aqueous LiCl, water, and brine and dried over anhydrous Na_2SO_4. After filtration and concentration, the residue was purified by flash chromatography (EtOAc/hexanes) to afford the desired methyl 5-(3,3-dimethylbut-1-ynyl)-3-((*R*)-4-methyl-*N*-((3*S*,6*s*)-1-oxaspiro[2.5]octan-6-yl)cyclohex-3-enecarboxamido)thiophene-2-carboxylate **56** as a white solid (2.70 g, 86% yield). ^{1}H NMR (400 MHz, DMSO-d_6): δ 7.33 (d, J = 18.9 Hz, 1H), 5.26 (br d, J = 17.2 Hz, 1H), 4.59−4.39 (m, 1H), 3.76 (d, J = 6.1 Hz, 3H), 2.55 (q, J = 4.8 Hz, 2H), 2.28−1.54 (m, 11H), 1.52 (s, 3H), 1.43−1.32 (m, 1H), 1.30 (d, J = 2.7 Hz, 9H), 1.17−0.93 (m, 3H).

Scheme 3, Steps f and g. **56** (2.69 g, 5.73 mmol) in THF (31 mL) and water (26 mL) was treated with lithium hydroxide (1.92 g, 46 mmol) with stirring at ambient temperature. After 16.5 h, the mixture was cooled to 0 °C and acidified to pH 4 with 10% citric acid (60 mL). The white cloudy mixture was extracted with ethyl acetate and washed with water and brine. After drying over anhydrous Na_2SO_4, the organic layer was filtered and concentrated to afford crude 5-(3,3-dimethylbut-1-ynyl)-3-((*R*)-4-methyl-*N*-((3*S*,6*s*)-1-oxaspiro[2.5]octan-6-yl)-cyclohex-3-enecarboxamido)thiophene-2-carboxylic acid as an off-white foam.

(*S*)-Tetrahydrofuran-3-ol (2.53 g, 28.7 mmol) in 1-methylpyrrolidin-2-one (19 mL) at 0 °C was treated portionwise with potassium *tert*-butoxide (2.57 g, 22.9 mmol) over 2 min. 5-(3,3-Dimethylbut-1-ynyl)-3-((*R*)-4-methyl-*N*-((3*S*,6*s*)-1-oxaspiro[2.5]octan-6-yl)cyclohex-3-enecarboxamido)thiophene-2-carboxylic acid (5.73 mmol) from the previous step was added in one portion, washing in the residue with 9 mL of 1-methylpyrrolidin-2-one. The mixture was warmed to 40 °C and stirred for 16 h. After cooling to 0 °C, the mixture was acidified to pH 3 with 2 M HCl, partitioned between ethyl acetate and water, and separated. The organic layer was washed with water and brine and dried over anhydrous Na_2SO_4. After filtration and removal of solvent under vacuum, the residue was purified by flash chromatography

dx.doi.org/10.1021/jm401420j | J. Med. Chem. XXXX, XXX, XXX−XXX

(EtOAc/dichloromethane) and recrystallized from warm acetonitrile/water to afford 5-(3,3-dimethylbut-1-ynyl)-3-((*R*)-*N*-((1*R*,4*S*)-4-hydroxy-4-(((*S*)-tetrahydrofuran-3-yloxy)methyl)cyclohexyl)-4-methylcyclohex-3-enecarboxamido)thiophene-2-carboxylic acid (**53**) as a white powder (1.96 g, 63% yield from **56**). MS (ESI$^+$) *m*/*z*: 544.0 [M + H]$^+$. ^{1}H NMR (400 MHz, DMSO-d_6): δ 13.49 (s, 1H), 7.18 (d, *J* = 18.3 Hz, 1H), 5.25 (d, *J* = 15.8 Hz, 1H), 4.39−4.23 (m, 1H), 4.10−4.01 (m, 1H), 3.99 (s, 1H), 3.76−3.56 (m, 4H), 3.13−3.00 (m, 2H), 2.25−1.96 (m, 2H), 1.96−1.33 (m, 18H), 1.29 (d, *J* = 2.7 Hz, 9H), 1.23−1.09 (m, 1H).

■ ASSOCIATED CONTENT

Ⓢ Supporting Information

Experimental details for the syntheses and spectroscopic characterization of the compounds in this paper and further assay details. This material is available free of charge via the Internet at http://pubs.acs.org.

Accession Codes

PDB code for HCV NS5B inhibitors: 4eo6.

■ AUTHOR INFORMATION

Corresponding Authors

*S.E.L.: phone, 650-522-1564; e-mail, scott.lazerwith@gilead.com.

*W.J.W.: phone, 650-522-5384; e-mail, will.watkins@gilead.com.

Present Addresses

[†]M.M.: Bristol-Myers Squibb Research and Development, P.O. Box 4000, Princeton, NJ 08543.

[‡]M.F.: Novartis Institutes for BioMedical Research, 4560 Horton Street, Emeryville, CA 94608.

[§]A.H.: Ironwood Pharmaceuticals, 301 Binney Street, Cambridge, MA 02142.

[∥]E.M.: Reset Therapeutics, 863A Mitten Road Suite 100C, Burlingame, CA 94010.

Notes

The authors declare the following competing financial interest(s): All of the authors of this manuscript are current or recent employees of Gilead Sciences.

■ ABBREVIATIONS USED

ACN, acetonitrile; AcOH, acetic acid; 9-BBN, 9-borabicyclo[3.3.1]nonane; CC_{50}, 50% cytostatic concentration; CCM, cell culture medium; Cmpd, compound; DIAD, diisopropyl azodicarboxylate; Et_3N, triethylamine; EtOAc, ethyl acetate; f_u, fraction unbound; GT, genotype; HCl, hydrochloric acid; HCV, hepatitis C virus; *i*-PrMgBr, isopropylmagnesium bromide; KHMDS, potassium hexamethyldisilazide; KO*t*-Bu, potassium *tert*-butoxide; LDA, lithium diisopropylamide; MeCN, acetonitrile; MeOH, methanol; min, minute; NaOAc, sodium acetate; NS, nonstructural; S_NAr, nucleophilic aromatic substitution; WT, wild type

■ REFERENCES

(1) Gane, E. J.; Stedman, C. A.; Hyland, R. H.; Ding, X.; Svarovskaia, E.; Symonds, W. T.; Hindes, R. G.; Berrey, M. M. Nucleotide Polymerase Inhibitor Sofosbuvir plus Ribavirin for Hepatitis C. *N. Engl. J. Med.* **2013**, *368*, 34−44.

(2) Poordad, F.; Lawitz, E.; Kowdley, K. V.; Cohen, D. E.; Podsadecki, T.; Siggelkow, S.; Heckaman, M.; Larsen, L.; Menon, R.; Koev, G.; Tripathi, R.; Pilot-Matias, T.; Bernstein, B. Exploratory Study of Oral Combination Antiviral Therapy for Hepatitis C. *N. Engl. J. Med.* **2013**, *368*, 45−53.

(3) Manns, M. P.; von Hahn, T. Novel therapies for hepatitis C—one pill fits all? *Nat. Rev. Drug Disc.* **2013**, *12*, 595−610.

(4) Watkins, W. J.; Ray, A. S.; Chong, L. HCV Polymerase Inhibitors. *Curr. Opin. Drug Discovery Dev.* **2010**, *13*, 441−465.

(5) Gopalsamy, A.; Lim, K.; Ciszewski, G.; Park, K.; Ellingboe, J. W.; Bloom, J.; Insaf, S.; Upeslacis, J.; Mansour, T. S.; Krishnamurthy, G.; Damarla, M.; Pyatski, Y.; Ho, D.; Howe, A. Y.; Orlowski, M.; Feld, B.; O'Connell, J. Discovery of Pyrano[3,4-*b*]indoles as Potent and Selective HCV NS5B Polymerase Inhibitors. *J. Med. Chem.* **2004**, *47*, 6603−6608.

(6) Chan, L.; Reddy, T. J.; Proulx, M.; Das, S. K.; Pereira, O.; Wang, W.; Siddiqui, A.; Yannopoulos, C. G.; Poisson, C.; Turcotte, N.; Drouin, A.; Alaoui-Ismaili, M. H.; Bethell, R.; Hamel, M.; L'Heureux, L.; Bilimoria, D.; Nguyen-Ba, N. Identification of N,N-Disubstituted Phenylalanines as a Novel Class of Inhibitors of Hepatitis C NS5B Polymerase. *J. Med. Chem.* **2003**, *46*, 1283−1285.

(7) Burton, G.; Ku, T. W.; Carr, T. J.; Kiesow, T.; Sarisky, R. T.; Lin-Goerke, J.; Baker, A.; Earnshaw, D. L.; Hofmann, G. A.; Keenan, R. M.; Dhanak, D. Identification of Small Molecule Inhibitors of the Hepatitis C Virus RNA-Dependent RNA Polymerase from a Pyrrolidine Combinatorial Mixture. *Bioorg. Med. Chem. Lett.* **2005**, *15*, 1553−1556.

(8) Li, H.; Tatlock, J.; Linton, A.; Gonzalez, J.; Borchardt, A.; Dragovich, P.; Jewell, T.; Prins, T.; Zhou, R.; Blazel, J.; Parge, H.; Love, R.; Hickey, M.; Doan, C.; Shi, S.; Duggal, R.; Lewis, C.; Fuhrman, S. Identification and Structure-Based Optimization of Novel Dihydropyrones as Potent HCV RNA Polymerase Inhibitors. *Bioorg. Med. Chem. Lett.* **2006**, *16*, 4834−4838.

(9) Nittoli, T.; Curran, K.; Insaf, S.; DiGrandi, M.; Orlowski, M.; Chopra, R.; Agarwal, A.; Howe, A. Y. M.; Prashad, A.; Brawner Floyd, M.; Johnson, B.; Sutherland, A.; Wheless, K.; Feld, B.; O'Connell, J.; Mansour, T. K.; Bloom, J. Identification of Anthranilic Acid Derivatives as a Novel Class of Allosteric Inhibitors of Hepatitis C NS5B Polymerase. *J. Med. Chem.* **2007**, *50*, 2108−2116.

(10) May, M. M.; Brohm, D.; Harrenga, A.; Marquardt, T.; Riedl, B.; Kreuter, J.; Zimmermann, H.; Ruebsamen-Schaeff, H.; Urban, A. Discovery of Substituted *N*-Phenylbenzenesulphonamides as a Novel Class of Non-Nucleoside Hepatitis C Virus Polymerase Inhibitors. *Antiviral Res.* **2012**, *95*, 182−191.

(11) LaPorte, M. G.; Draper, T. L.; Miller, L. E.; Blackledge, C. W.; Leister, L. K.; Amparo, E.; Hussey, A. R.; Young, D. C.; Chunduru, S. K.; Benetatos, C. A.; Rhodes, G.; Gopalsamy, A.; Herbertz, T.; Burns, C. J.; Condon, S. M. The Discovery and Structure−Activity Relationships of Pyrano[3,4-*b*]indole Based Inhibitors of Hepatitis C Virus NS5B Polymerase. *Bioorg. Med. Chem. Lett.* **2010**, *20*, 2968−2973.

(12) Jackson, R. W.; LaPorte, M. G.; Herbertz, T.; Draper, T. L.; Gaboury, J. A.; Rippin, S. R.; Patel, R.; Chunduru, S. K.; Benetatos, C. A.; Young, D. C.; Burns, C J.; Condon, S. M. The Discovery and Structure−Activity Relationships of Pyrano[3,4-*b*]indole-Based Inhibitors of Hepatitis C Virus NS5B Polymerase. *Bioorg. Med. Chem. Lett.* **2011**, *22*, 3227−3231.

(13) Chan, L.; Das, S. K.; Reddy, T. J.; Poisson, C.; Proulx, M.; Pereira, O.; Courchesne, M.; Roy, C.; Wang, W.; Siddiqui, A.; Yannopoulos, C. G.; Nguyen-Ba, N.; Labrecque, D.; Bethell, R.; Hamel, M.; Courtemanche-Asselin, P.; L'Heureux, L.; Maud, D.; Nicolas, O.; Brunette, S.; Bilimoria, D.; Bédard, J. Discovery of Thiophene-2-carboxylic Acids as Potent Inhibitors of HCV NS5B Polymerase and HCV Subgenomic RNA Replication. Part 1: Sulfonamides. *Bioorg. Med. Chem. Lett.* **2004**, *14*, 793−796.

(14) Chan, L.; Pereira, O.; Reddy, T. J.; Das, S. K.; Poisson, C.; Courchesne, M.; Proulx, M.; Siddiqui, A.; Yannopoulos, C. G.; Nguyen-Ba, N.; Roy, C.; Nasturica, D.; Moinet, C.; Bethell, R.; Hamel, M.; L'Heureux, L.; Maud, D.; Nicolas, O.; Courtemanche-Asselin, P.; Brunette, S.; Bilimoria, D.; Bédard, J. Discovery of Thiophene-2-carboxylic Acids as Potent Inhibitors of HCV NS5B Polymerase and HCV Subgenomic RNA Replication. Part 2: Tertiary Amides. *Bioorg. Med. Chem. Lett.* **2004**, *14*, 797−800.

(15) Slater, M. J.; Amphlett, E. M.; Andrews, D. M.; Bravi, G.; Burton, G.; Cheasty, A. G.; Corfield, J. A.; Ellis, M. R.; Fenwick, R. H.; Fernandes, S.; Guidetti, R.; Haigh, D.; Hartley, C. D.; Howes, P. D.; Jackson, D. L.; Jarvest, R. L.; Lovegrove, V. L.; Medhurst, K. J.; Parry, N. R.; Price, H.; Shah, P.; Singh, O. M.; Stocker, R.; Thommes, P.; Wilkinson, C.; Wonacott, A. Optimization of Novel Acyl Pyrrolidine Inhibitors of Hepatitis C Virus RNA-Dependent RNA Polymerase Leading to a Development Candidate. *J. Med. Chem.* **2007**, *50*, 897−900.

(16) Li, H.; Tatlock, J.; Linton, A.; Gonzalez, T.; Jewell, T.; Patel, L.; Ludlum, S.; Drowns, M.; Rahavendran, S. V.; Skor, H.; Hunter, R.; Shi, S. T.; Herlihy, K. J.; Parge, H.; Hickey, M.; Yu, X.; Chau, F.; Nonomiya, J.; Lewis, C. Discovery of (*R*)-6-Cyclopentyl-6-(2-(2,6-diethylpyridin-4-yl)ethyl)-3-((5,7-dimethyl-[1,2,4]triazolo[1,5-*a*]-pyrimidin-2-yl)methyl)-4-hydroxy-5,6-dihydropyran-2-one (PF-00868554) as a Potent and Orally Available Hepatitis C Virus Polymerase Inhibitor. *J. Med. Chem.* **2009**, *52*, 1255−1258.

(17) Ontoria, J. M.; Rydberg, E. H.; Di Marco, S.; Tomei, L.; Attenni, B.; Malancona, S.; Martin Hernando, J. I.; Gennari, N.; Koch, U.; Narjes, F.; Rowley, M.; Summa, V.; Olsen, D. B.; De Francesco, R.; Altamura, S.; Migliaccio, G.; Carfì, A. Identification and Biological Evaluation of a Series of 1*H*-Benzo[*de*]isoquinoline-1,3(2*H*)-diones as Hepatitis C Virus NS5B Polymerase Inhibitors. *J. Med. Chem.* **2009**, *52*, 5217−5227.

(18) Beaulieu, P. L.; Coulombe, R.; Duan, J.; Fazal, G.; Godbout, C.; Hucke, O.; Jakalian, A.; Joly, M. A.; Lepage, O.; Llinàs-Brunet, M.; Naud, J.; Poirier, M.; Rioux, N.; Thavonekham, B.; Kukolj, G.; Stammers, T. A. Structure-Based Design of Novel HCV NS5B Thumb Pocket 2 Allosteric Inhibitors with Submicromolar GT1 Replicon Potency: Discovery of a Quinazolinone Chemotype. *Bioorg. Med. Chem. Lett.* **2013**, *23*, 4132−4140.

(19) Statement on a Nonproprietary Name Adopted by the USAN Council. http://www.ama-assn.org/resources/doc/usan/lomibuvir.pdf.

(20) Hucke, O.; Coulombe, R.; Bonneau, P.; Bertrand-Laperle, M.; Brochu, C.; Gillard, J.; Joly, M. A.; Landry, S.; Lepage, O.; Llinàs-Brunet, M.; Pesant, M.; Poirier, M.; Poirier, M.; McKercher, G.; Marquis, M.; Kukolj, G.; Beaulieu, P. L.; Stammers, T. A. Molecular Dynamics Simulations and Structure-Based Rational Design Lead to Allosteric HCV NS5B Polymerase Thumb Pocket 2 Inhibitor with Picomolar Cellular Replicon Potency. *J. Med. Chem.* [Online early access]. DOI: 10.1021/jm4004522. Published Online: June 17, **2013**.

(21) Wagner, P.; Thompson, R.; Kantaridis, C.; Simpson, P.; Troke, P. J. F.; Jagannatha, S.; Neelakantan, S.; Purohit, V. S.; Hammond, J. L. Antiviral Activity of the Hepatitis C Virus Polymerase Inhibitor Filibuvir in Genotype 1-Infected Patients. *Hepatology* **2011**, *54*, 50−59.

(22) Cooper, C.; Larouche, R.; Bourgault, B.; Chauret, N.; Proulx, L. Safety, Tolerability and Pharmacokinetics of the HCV Polymerase Inhibitor VCH-222 following Single Dose Administration in Healthy Volunteers and Antiviral Activity in HCV-Infected Individuals. *J. Hepatol.* **2009**, *50* (S1), S342.

(23) Robinson, M.; Yang, H.; Sun, S. C.; Peng, B.; Tian, Y.; Pagratis, N.; Greenstein, A. E.; Delaney, W. E. Novel Hepatitis C Virus Reporter Replicon Cell Lines Enable Efficient Antiviral Screening against Genotype 1a. *Antimicrob. Agents Chemother.* **2010**, *54*, 3099−3106.

(24) Lohmann, V. F.; Korner, J. K.; Herian, U.; Theilmann, L.; Bartenschlager, R. Replication of Subgenomic Hepatitis C Virus RNAs in a Hepatoma Cell Line. *Science* **1999**, *285*, 110−113.

(25) Fenaux, M.; Eng, S.; Leavitt, S. A.; Lee, Y. J.; Mabery, E. M.; Tian, Y.; Byun, D.; Canales, E.; Clarke, M. O.; Doerffler, E.; Lazerwith, S. E.; Lew, W.; Liu, Q.; Mertzman, M.; Morganelli, P.; Xu, L.; Ye, H.; Zhang, J.; Matles, M.; Murray, B. P.; Mwangi, J.; Zhang, J.; Hashash, A.; Krawczyk, S. H.; Bidgood, A. M.; Appleby, T. C.; Watkins, W. J. Preclinical Characterization of GS-9669, a Thumb Site II Inhibitor of the Hepatitis C Virus NS5B Polymerase. *Antimicrob. Agents Chemother.* **2013**, *57*, 804−810.

(26) Wunberg, T.; Baumeister, J.; Gottchling, D.; Henninger, K.; Koletzki, D.; Pernerstorfer, J.; Urban, A.; Birkmann, A.; Harrenga, A.; Lobell, M. Alkinyl-Substituted Thiophenes. WO 2006/07234, 2006.

(27) Chiral HPLC analysis of several compounds containing asymmetric centers on the *N*-alkyl or *N*-acyl substituents showed no evidence that these apparent atropisomers were separable.

(28) LaPlant, S. R.; Forgione, P.; Boucher, C.; Coulombe, R.; Gillard, J.; Hucke, O.; Jakalian, A.; Joly, M.-A.; Kukolj, G.; Lemke, C.; McCollum, R.; Titolo, S. Enantiomeric Atropisomers Inhibit HCV Polymerase and/or HIV Matrix: Characterizing Hindered Bond Rotations and Target Selectivity. *J. Med. Chem.* [Online early access]. DOI: 10.1021/jm401202a. Published Online: Sep 11, **2013**.

(29) Canales, E.; Carlson, J. S.; Appleby, T.; Fenaux, M.; Lee, J.; Tian, Y.; Tirunagari, N.; Wong, M.; Watkins, W. J. Tri-Substituted Acylhydrazines As Tertiary Amide Bioisosteres: HCV NS5B Polymerase Inhibitors. *Bioorg. Med. Chem. Lett.* **2012**, *22*, 4288−4292.

(30) Yang, H.; Hendricks, R. T.; Arora, N.; Nitzan, D.; Yee, C.; Lucas, M. C.; Yang, Y.; Fung, A.; Rajyaguru, S.; Harris, S. F.; Leveque, V. J.; Hang, J. Q.; Pogam, S. L.; Reuter, D.; Tavares, G. A. Cyclic Amide Bioisosterism: Strategic Application to the Design and Synthesis of HCV NS5B Polymerase Inhibitors. *Bioorg. Med. Chem. Lett.* **2010**, *20*, 4614−4619.

(31) Lai, V. C. H.; Dempsey, S.; Lau, J. Y. N.; Hong, Z.; Zhong, W. In Vitro RNA Replication Directed by Replicase Complexes Isolated from the Subgenomic Replicon Cells of Hepatitis C Virus. *J. Virol.* **2003**, *77*, 2295−2300.

(32) Seyferth, D.; Marmor, R. S.; Hilbert, P. Reactions of Dimethylphosphono-Substituted Diazoalkanes. $(MeO)_2P(O)CR$ Transfer to Olefins and 1,3-Dipolar Additions of $(MeO)_2P(O)C(N_2)$-R. *J. Org. Chem.* **1971**, *36*, 1379−1386.

(33) Müller, S.; Liepold, B.; Roth, G.; Bestmann, H. J. An Improved One-Pot Procedure for the Synthesis of Alkynes from Aldehydes. *Synlett* **1996**, 521−522.

(34) Barnes-Seeman, D.; Monish, J.; Bell, L.; Ferreira, S.; Cohen, S.; Chen, X.-H.; Amin, J.; Snodgrass, B.; Hatsis, P. Metabolically Stable *tert*-Butyl Replacement. *ACS Med. Chem. Lett.* **2013**, *4*, 514−516.

(35) Wang, M.; Ng, K. K.; Cherney, M. M.; Chan, L.; Yannopoulos, C. G.; Bedard, J.; Morin, N.; Nguyen-Ba, N.; Alaoui-Ismaili, M. H.; Bethell, R. C.; James, M. N. Non-Nucleoside Analogue Inhibitors Bind to an Allosteric Site on HCV NS5B Polymerase. Crystal Structures and Mechanism of Inhibition. *J. Biol. Chem.* **2003**, *278*, 9489−9495.

(36) Leung, C. S.; Leung, S. S.; Tirado-Rives, J.; Jorgensen, W. L. Methyl Effects on Protein−Ligand Binding. *J. Med. Chem.* **2012**, *55*, 4489−4500.

(37) (*R*)-4-Methylcyclohex-3-enecarboxylic acid was prepared according to the procedure for the synthesis of (*S*)-4-methylcyclohex-3-enecarboxylic acid found in Poll, T.; Sobczak, A.; Hartmann, H.; Helmchen, G. *Tetrahedron Lett.***1985**, *26*, 3095−3098, using (*S*)-pantolactone in place of (*R*)-pantolactone.

(38) Lawitz, E.; Hazan, L.; Gruener, D.; Hack, H.; Backonja, M.; Hill, J.; German, P.; Dvory-Sobol, H.; Jain, A.; Arterburn, S.; Watkins, W. J.; Rossi, S.; McHutchison, J.; Rodriguez-Torres, M. GS-9669, a Novel NS5B Non-Nucleoside Thumb Site II Inhibitor, Demonstrates Potent Antiviral Activity, Favorable Safety Profile and Potential for Once-Daily Dosing. *J. Hepatol.* **2012**, *56* (S2), S471.